Resonant Optical Interactions with Molecules Confined in Photonic Band-Gap Fibers

Saikat Ghosh, Jay E. Sharping, Dimitre G. Ouzounov, and Alexander L. Gaeta*
School of Applied and Engineering Physics, Cornell University, Ithaca, NY 14853, USA
(Received 2 December 2004; published 11 March 2005)

We investigate resonant nonlinear optical interactions and demonstrate induced transparency in acetylene molecules in a hollow-core photonic-band-gap fiber at 1.5 μm. The induced spectral transmission window is used to demonstrate slow-light effects, and we show that the observed broadening of the spectral features is due to collisions of the molecules with the inner walls of the fiber core. Our results illustrate that such fibers can be used to facilitate strong coherent light-matter interactions even when the optical response of the individual molecules is weak.

DOI: 10.1103/PhysRevLett.94.093902 PACS numbers: 42.70.Qs, 32.80.Qk, 42.50.Gy, 42.65.Wi

The fields of photonics and quantum optics have undergone immense technological and scientific advancement in the past decade. The growth of the telecommunications industry has given rise to exotic devices such as the hollow-core photonic-band-gap fiber (HC-PBF) [1,2], which can guide light over hundreds of meters through a hollow-core surrounded by a photonic crystal structure (see Fig. 1) that localizes light in the core. In addition, since the nonlinearities are determined primarily by the gas in the fiber's core, such fibers can be used to produce efficient Raman scattering [3,4] and solitons with megawatt powers [5].

In parallel with these developments, there has been tremendous progress in the field of coherent atom-photon interactions. The richness of physics in manipulating quantum states of matter and creating coherent superpositions has led to numerous studies in atom cooling and Bose-Einstein condensation [6], quantum information and computation [7–9], and electromagnetically induced transparency (EIT) [10,11]. In particular, the phenomenon of EIT has led to an assortment of potentially practical applications such as ultra-slow light [12,13], light storage in a medium [14], and single-photon switching [15,16]. Our research is motivated by the desire to integrate novel photonic devices [17,18] with coherent atom-photon interactions and to build useful devices for the fields of telecommunications and quantum information processing. Hollow-core photonic-band-gap fiber, with the ability to confine atoms and molecules to its core for extremely long interaction lengths and to integrate itself readily with the existing telecommunication technology, seems to be the ideal bridge between photonics and quantum optics.

In this Letter, we describe experiments that represent the first demonstration of coherent resonant interactions in these fibers. We perform coherent three-level spectroscopy of acetylene molecules confined to the core of a HC-PBF. Using a strong control beam to modify coherently a three-level molecular system, we observe induced transparencies of the probe beam as large as 50% and we demonstrate slow-light delays via this transparency window. These results indicate that such fibers can be used to greatly enhance light-matter interactions even when the optical response of the individual molecules is weak.

The use of acetylene for optical interactions has attracted significant interest due to its spectral overlap with the low-loss C-band fiber telecommunications window [19]. In addition, several low-loss HC-PBF have been demonstrated with band gaps in this spectral range [2]. This motivates us to study coherence effects in acetylene (C_2H_2), a linear symmetric molecule, which has clean rovibrational transitions [20] in this wavelength range [21]. Only a few studies have demonstrated coherence effects in molecular systems [22,23], and one of the primary reasons is due to the typically weak oscillator strengths of the molecular transitions. Observation of an appreciable effect in a bulk molecular gas necessitates the opposing requirement of a tightly focused laser beam and a long interaction length. While the effective interaction between the optical field and the molecular system can be enhanced by using an optical cavity or a capillary tube, the small core diame-

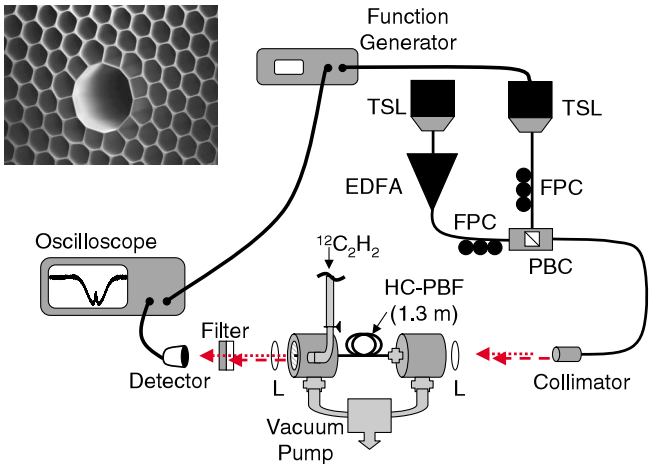

FIG. 1 (color online). Schematic diagram of the experimental setup. The transverse cross section of the HC-PBF is also shown. EDFA: erbium-doped fiber amplifier; TSL: tunable semiconductor laser; FPC: fiber-polarization controller; PBC: polarization-beam combiner; L: lens.

ter of the HC-PBF, together with practically lossless propagation of fields over many meters, provides a superior alternative. A discussion of the advantages of HC-PBF over capillary tubes is given by Benabid *et al.* [3].

In our experiments we use a 1.33-m-long HC-PBF (Blazephotonics, HC-1550-01) which has a core diameter of 12 μm and a band gap extending from 1490–1620 nm. As shown in Fig. 1, the two ends of the fiber are placed in separate vacuum cells. During assembly, we purge the air inside the fiber using nitrogen gas and then evacuate to a pressure below 10^{-6} Torr. One of the cells is then filled with 99.8% pure C_2H_2. We detect the presence of the gas in the other cell spectroscopically to ensure that the core is filled with acetylene. All experiments are performed in steady state with both of the cells at the same pressure, which ranges from 10–200 mTorr. For the fiber used in these measurements, steady state is reached in less than an hour.

We use two tunable external-cavity lasers for pump-probe spectroscopy. The emission from one of the lasers is tuned to 1535 nm and amplified by a 1-W erbium-doped fiber amplifier (EDFA). We use the amplified beam as our control beam. The other laser is tuned to 1517 nm and serves as the probe beam. The control and probe beams are combined using fiber-polarization controllers and a polarization-beam combiner. The copropagating control and probe beams are collimated and then launched into one end of the fiber with coupling efficiencies of 50% using a microscope objective. We filter out the control beam from the probe using an interference filter with a rejection ratio of >50 dB, and the probe is detected by a photodetector.

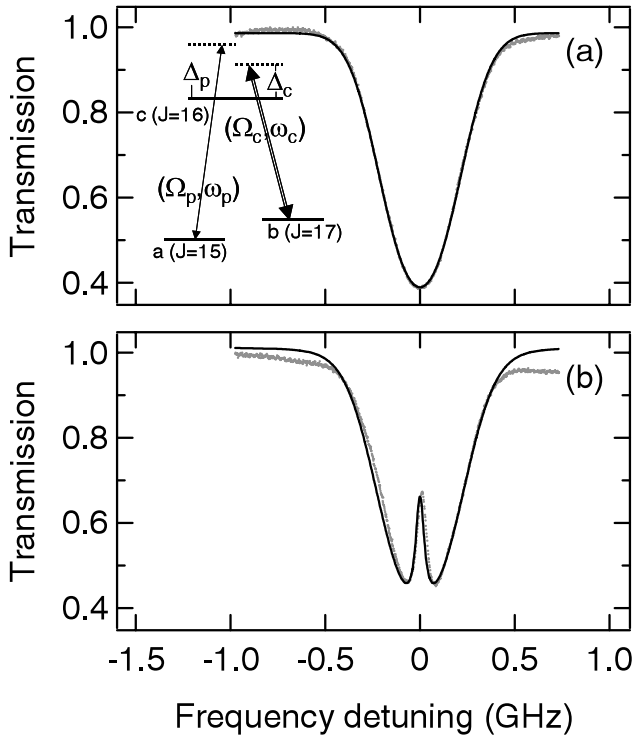

FIG. 2. (a) Measured (points) and theoretical (line) Doppler-broadened absorption spectra for the $R(15)$ transition in acetylene within a 1.3-m segment of photonic-band-gap fiber. A diagram of the relevant molecular levels is shown in the inset. (b) Measured (points) and theoretical (line) spectra for the same transition in the presence of a strong control beam (320 mW at the fiber output).

The energy-level scheme for the molecules used in our experiment is shown in Fig. 2. The control beam is tuned between the levels $0(\Sigma_g^+)(J = 17)$ and $\nu_1 + \nu_3(\Sigma_u^+)(J = 16)$, denoted as levels b and c, respectively. The probe beam is tuned between level a, which is $0(\Sigma_g^+)(J = 15)$, and c. These are the $P(17)$ and $R(15)$ lines of $^{12}C_2H_2$ at 1535.3927 nm and 1517.3144 nm, respectively [20]. The probe power is maintained below 500 μW, and the wavelength of the probe is scanned over the $R(15)$ transition line. As shown in Fig. 2(a), without the control beam we observe the Doppler-broadened absorption of the probe beam with a width of 480 MHz. In the presence of the control beam, a transparency window is opened. Figure 2(b) shows a typical trace of the probe-field absorption of the $R(15)$ line in presence of a 320-mW (measured at the output of the fiber) control beam tuned exactly to the center of the $P(17)$ transition. While induced transparencies of this magnitude have been observed routinely in focused geometries in atomic systems such as rubidium, observing this transparency feature in acetylene is remarkable in light of the fact that the oscillator strength of the transition is several orders of magnitude less than that for the D lines of rubidium transitions.

For an understanding of our experimental results, we solve the density matrix equations for a three-level Λ system (see Fig. 2), where one of the two lower levels, (J_b, m), is coupled to the upper level (J_c, m) with a strong control field E_c, while the transition $(J_a, m) - (J_c, m)$ is probed with a weak field E_p. Here m is the orientational quantum number, denoting the alignment of the otherwise degenerate ro-vibrational levels. We first calculate the steady-state population distribution for the three-level system in presence of the strong control field and no probe field [24]. We consider a semi-open system, where the upper level radiatively decays to the two lower levels with a decay rate (γ) independent of m. We further consider a collisional redistribution of population between the two lower levels at a rate $w_{ab} = w_{ba}$. We use the resulting steady-state population expressions $\rho_{ii}^{m(0)}$ for levels $i = a, b, c$ to calculate the coherence ρ_{ca}^m correct to first order in the probe field,

$$\rho_{ca}^m = \frac{-i\Omega_p^m}{2(\gamma_{ca} - i\Delta_p + \frac{|\Omega_c^m|^2/4}{\gamma_{ba} - i(\Delta_p - \Delta_c)})}\Bigg[(\rho_{cc}^{m(0)} - \rho_{aa}^{m(0)}) + \frac{|\Omega_c^m|^2}{4(\gamma_{cb} + i\Delta_c)[\gamma_{ba} - i(\Delta_p - \Delta_c)]}(\rho_{bb}^{m(0)} - \rho_{cc}^{m(0)})\Bigg], \quad (1)$$

where $\Delta_c = \omega_c - \omega_{cb} - k_c v$ and $\Delta_p = \omega_p - \omega_{ca} - k_p v$ are the velocity-dependent detunings of the control and the probe field, with wave vectors, k_c and k_p, respectively, and Ω_c^m is the Rabi frequency of the control field, which can be expressed as

$$\Omega_c^m = \frac{2\langle \Sigma_u^+(J_c, m) \mid \hat{\mu} \mid \Sigma_g^+(J_b, m)\rangle E_c}{\hbar} = \frac{2\mu^0 F^0_{\Sigma-\Sigma}(J_c, m; J_b, m) E_c}{\hbar}, \quad (2)$$

where μ^0 is the pure electronic-vibrational transition dipole moment, and $F^0_{\Sigma-\Sigma}(J_c, m; J_a, m)$ is the Hönl-London factor for the transition [25]. Similarly, Ω_p^m is the Rabi frequency associated with the probe field. The control and probe beams are assumed to be copolarized. Equation (1) reduces to the usual EIT coherence for a closed three-level system, with the approximation of $\rho_{aa}^{m(0)} \simeq 1$, $\rho_{bb}^{m(0)} = \rho_{cc}^{m(0)} \simeq 0$. The first term inside the brackets contributes to saturation of the transition $(J_b, m) - (J_c, m)$ due to the presence of the control field with powers above the saturation intensity [26], and the second term represents an interference due to the oscillation of population between $(J_b, m) - (J_c, m)$.

The dephasing rates are expressed in the form, $\gamma_{ij} = (\gamma_i + \gamma_j)/2 + \gamma_{ij}^{\text{coll}}$, for $i = a, b, c$, where γ_i is the decay rate of level i and $\gamma_{ij}^{\text{coll}}$ is the dephasing rate due to collision of the molecules with each other and with the inside wall of the HC-PBG fiber. Following Ref. [27], an estimate for the pressure-broadened lifetimes for these transitions of C_2H_2 at wavelengths of 1.5 μm is of the order of 10 MHz/Torr. At our working pressures near 50 mTorr, the linewidth is estimated to be less than 1 MHz. In contrast, an estimate of the linewidth due to dephasing collisions with the inside walls of the fiber, assuming a mean thermal velocity of the molecules of 400 m/sec inside a cylinder of diameter 12 μm, predicts a value which is an order of magnitude larger. We expect these collisions to be the major source of decoherence in our system. The dephasing rate γ_{ij} is therefore assumed to be the same for all coherences, with $\gamma_{ij}^{\text{coll}} = \gamma_{\text{wall}}^{\text{coll}}$.

To compare our experiment with theory, we first average the coherence over the Doppler profile and sum over the orientation (m) to obtain the probe-field susceptibility χ, and we fit our experimental data to the transmission coefficient

$$T = \frac{I_{\text{out}}}{I_{\text{in}}} = \exp[-4\pi k_p L \text{Im}\{\chi\}], \quad (3)$$

where L is the length of the fiber. In Eq. (3), we assume the Rabi frequency for the control field is constant along the length of the fiber.

The variable parameters in the theory are: (i) the constant term in the exponent of Eq. (3), which is the product of the number density, the length of the fiber, and the constants for the Rabi frequency of the probe-field, (ii) the collisional redistribution rate of the ground-state population w_{ab}, (iii) the pure electronic-vibrational Rabi strength $\Omega_c^0 = 2\mu^0 E_c/\hbar$, (iv) the upper-state decay rate 2γ, and (v) the dephasing rate $\gamma_{\text{coll}}^{\text{wall}}$ due to collisions with the inside walls of the fiber. We first estimate the constant for (i) for the probe field by fitting the Doppler-broadened probe-field absorption without the control field [Fig. 2(a)]. The relative height of the probe-field absorption, with and without the control field, depends primarily on the rate w_{ab}. A choice of $w_{ab} = 0.4\gamma$ matches well with all our experimental absorption curves over the entire range of the control-field strength. We fit the remaining parameters, Ω_c^0, γ, and $\gamma_{\text{coll}}^{\text{wall}}$ to the experimental data. We make an initial guess of Ω_c^0 by estimating E_c from the input control-field power in the fiber and using the values for μ^0 from Ref. [28]. For γ we use an estimate from Ref. [27], and our initial guess for $\gamma_{\text{coll}}^{\text{wall}}$ is as discussed above.

As seen in Fig. 2(b), our theoretical model is in excellent agreement with our experimentally measured probe-field absorption. Our value for $\Omega_c^0 = 9.3$ MHz is consistent with the measured control power of 320 mW, and a value of $\gamma = 0.96$ MHz and $\gamma_{\text{wall}}^{\text{coll}} = 17.28$ MHz is estimated

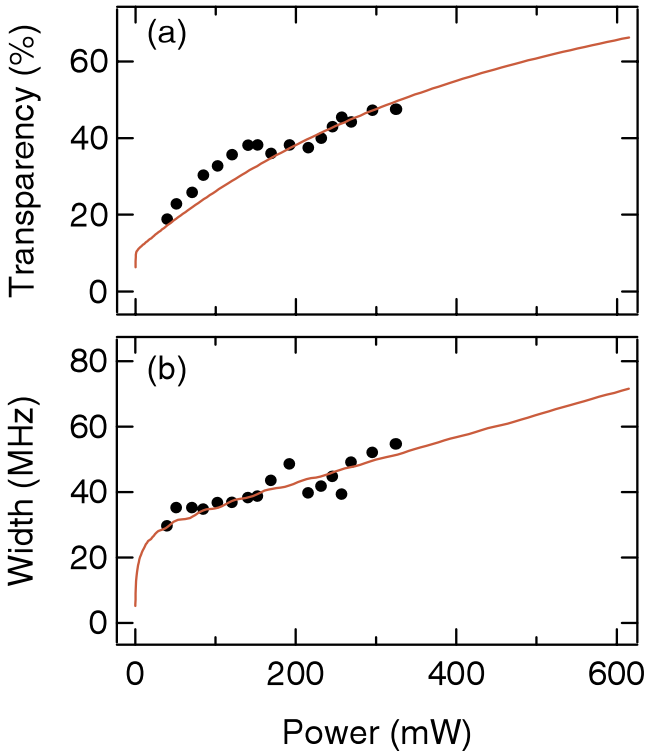

FIG. 3 (color online). (a) Experimental (circles) and theoretical (lines) relative transparencies (ratio of the change in the zero-detuning probe transmission in the presence of the control beam to the zero-detuning probe transmission without the control beam) as functions of control power measured at the output of the fiber. (b) The corresponding width (FWHM) of the transparency dip.

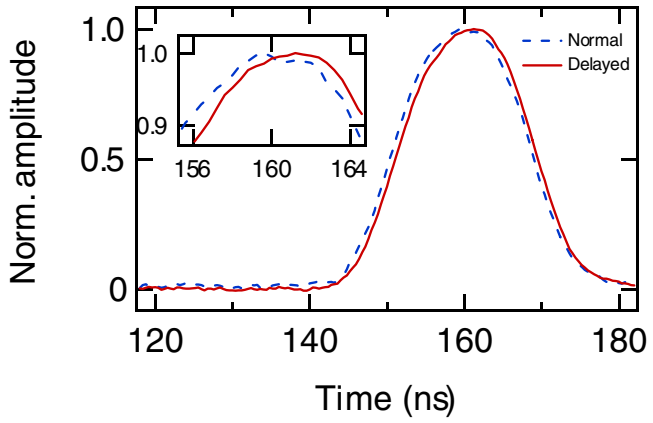

FIG. 4 (color online). Normalized amplitude vs time for a probe pulse with (delayed) and without (normal) the control beam. The inset shows a close-up of the pulse peaks. See text for measurement details.

from the fit. Figure 3(a) shows a plot of the transparency as a function of the control power measured at the output end of the fiber together with the corresponding theoretical plot. Presently in our experiments, we are limited by the power of our amplifiers for the control field, but theory predicts a much larger transparency at higher powers. The measured transparency full-width at half maximum (FWHM) in Fig. 3(b) shows a linear dependence on control power, which has the behavior of the EIT linewidth $\Gamma_{\mathrm{EIT}} \Rightarrow \Omega_c^{02}$ of Ref. [24].

An interesting application of our system, which has relevance to both telecommunications and quantum information, is to use this spectroscopic feature to produce a delay whose magnitude can be varied by controlling the width of the resonance [Fig. 3(b)]. Sharp changes in the absorption of a probe field due to coherent effects produced by a strong control field are accompanied by dramatic changes in the refractive index [12,13]. As a proof of concept, we generate 19-ns (FWHM) probe pulses using an amplitude modulator and tune the wavelength of the probe to be on resonance with the a-c transition. The wavelength of the copropagating cw control beam is tuned to be on resonance with the b-c transition. The control beam is filtered using a tunable bandpass filter, and the probe pulses are detected with a 10-GHz receiver. For these measurements the control beam power measured at the output of the fiber is 200 mW, and the on-resonance probe absorption and relative transparency are both approximately 40%. Figure 4 shows the probe pulse with the control beam off and with it on. The delay measured in the presence of the control beam is 800 ps. This represents, to our knowledge, the first demonstration of slow light at telecommunications wavelengths using molecular spectroscopic features.

In summary, we have investigated coherent three-level resonant interactions with acetylene molecules inside a HC-PBF. A theoretical model was used to estimate the effect of decoherence due to collision of the molecules with the inside wall of the fiber. We used this spectroscopic feature to demonstrate a potential application of producing slow light with molecules inside optical fibers at telecommunication wavelengths.

We thank K. Moll, K. Koch, and D. Gauthier for useful discussions and comments. We gratefully acknowledge support by the Center for Nanoscale Systems, supported by the NSF under Grant No. EEC-0117770, the Air Force Office of Scientific Research under Contract No. F49620-03-0223, and DARPA under the Slow-Light program.

*Electronic address: a.gaeta@cornell.edu

[1] R. F. Cregan *et al.*, Science **285**, 1537 (1999).
[2] C. M. Smith *et al.*, Nature (London) **424**, 657 (2003).
[3] F. Benabid *et al.*, Science **298**, 399 (2002).
[4] F. Benabid *et al.*, Phys. Rev. Lett. **93**, 123903 (2004)
[5] D. G. Ouzounov *et al.*, Science **301**, 1702 (2003).
[6] M. H. Anderson *et al.*, Science **269**, 198 (1995).
[7] *The Physics of Quantum Information: Quantum Cyrptograpy, Teleportation, and Quantum Computation*, edited by D. Bouwmeester *et al.* (Springer, New York, 2000).
[8] M. D. Lukin, Rev. Mod. Phys. **75**, 457 (2003).
[9] R. G. Beausoleil *et al.*, J. Mod. Opt. **51**, 1559 (2004).
[10] O. A. Kocharovskaya and Y. I. Khanin, JETP Lett. **48**, 630 (1988).
[11] S. E. Harris, Phys. Rev. Lett. **62**, 1033 (1989).
[12] C. Liu *et al.*, Nature (London) **409**, 490 (2001).
[13] M. M. Kash *et al.*, Phys. Rev. Lett. **82**, 5229 (1999).
[14] D. F. Phillips *et al.*, Phys. Rev. Lett. **86**, 783 (2001).
[15] H. Schmidt and A. Imamoglu, Opt. Lett. **21**, 1936 (1996).
[16] S. E. Harris and Y. Yamamoto, Phys. Rev. Lett. **81**, 3611 (1998).
[17] D. Yin, H. Schmidt, J. P. Barber, and A. R. Hawkins, Opt. Express **12**, 2710 (2004).
[18] M. Soljačić *et al.*, physics/0406001.
[19] W. C. Swann and S. L. Gilbert, J. Opt. Soc. Am. B **17**, 1263 (2000).
[20] K. A. Keppler *et al.*, J. Mol. Spectrosc. **175**, 411 (1996).
[21] T. Ritari *et al.*, Opt. Express **12**, 4080 (2004).
[22] J. Qi *et al.*, Phys. Rev. Lett. **83**, 288 (1999).
[23] J. Qi *et al.*, Phys. Rev. Lett. **88**, 173003 (2002).
[24] A. Javan *et al.*, Phys. Rev. A **66**, 013805 (2002).
[25] F. C. Spano, J. Chem. Phys. **114**, 276 (2001).
[26] H. R. Schlossberg and A. Javan, Phys. Rev. **150**, 267 (1966).
[27] M. deLabachelerie *et al.*, Opt. Lett. **19**, 840 (1994).
[28] R. El. Hachtouki and J. V. Auwera, J. Mol. Spectrosc. **216**, 355 (2002).